ELSEVIER

Catalysis Today 65 (2001) 265–270

CATALYSIS TODAY

www.elsevier.com/locate/cattod

Mixed oxides as a support for new CoMo catalysts

C. Flego*, V. Arrigoni, M. Ferrari, R. Riva, L. Zanibelli

EniTecnologie SpA-Via Maritano, 26-S. Donato Mil. (MI) 20097, Italy

Abstract

Interest in bifunctional catalysts, active in reactions such as hydrodesulphurisation (HDS) of hydrocarbon fractions, is growing in the last years. An improvement of $CoMo/Al_2O_3$ materials can be obtained by the introduction of other oxides during the sol–gel synthesis. This heavily affects the acid–base characteristics of the catalysts, while textural properties are less influenced. The catalytic performances change as well: a relationship between the density of acid sites and HDS activity has been found. © 2001 Elsevier Science B.V. All rights reserved.

Keywords: CoMo catalysts; Hydrodesulphurisation; Sol–gel synthesis; Mixed oxides

1. Introduction

Restrictive environmental regulations are pushing the development of more efficient hydrotreating technologies, able to decrease the content of heteroatoms in the different oil cuts. Since gasoline obtained by fluid-catalytic cracking (FCC) contains ca. 95% of the total S present in the overall gasoline pool, its processing produces results of fundamental interest. Thiophene and its alkyl derivatives represent ca. 60% of sulphur compounds in gasoline, the remainder being mercaptans and sulfides [1].

Bifunctional catalysts, active in reactions such as hydrodesulphurisation (HDS), are based on supported metal sulphides (MoS_2, WS_2) and promoters (Co, Ni). The most commonly used support for these catalysts is alumina. New generations of HDS catalysts involve: (i) traditional formulation prepared through new optimised procedures, (ii) improved compositions. The textural properties as well as the acid–base character of alumina can be modified by addition of other oxides [2,3]. Changing the support composition is considered as a promising line of research to achieve higher hydrotreating performances [4–6,20]. The aim of this work is to evaluate the influence of the addition of oxides (Zr, Ga, Si, B) on the physico-chemical characteristics of alumina based supports and the corresponding CoMo catalysts, prepared by the sol–gel method. The catalytic performances in HDS of thiophene are also studied.

2. Experimental

2.1. Catalyst and support preparation

The mixed oxide supports and the corresponding CoMo catalysts were synthesised according to [7], following the sol–gel procedure [8].

Al_2O_3 based supports: Precursors of different oxides (M = Zr, Ga, Si, B) were dissolved in butanol (isopropanol in the case of $Zr(OC_3H_7)_4$, 70 wt.%); then aluminium *sec*-butoxide $Al(OC_4H_9)_3$ was added, heated and kept at 60°C for about 20 min. An aqueous solution containing TPAOH

* Corresponding author. Fax: +39-0252056364.
E-mail address: cflego@enitecnologie.eni.it (C. Flego).

0920-5861/01/$ – see front matter
PII: S0920-5861(00)00560-5

(tetrapropylammonium-hydroxide) was added slowly to the alcoholic solution, while heating at 80°C. After 1 h the gel was formed, then aged at 21°C, dried (6 h, 100°C, in vacuum) and calcined (3 h, 550°C, air flow). The resulting M/Al molar ratio was 0.1, except for ZA, where Zr/Al was 0.15.

CoMo catalysts: $Co(NO_3)_2{\cdot}6H_2O$ was dissolved in $CH_3(CH_2)_3OH$ or *i*-PrOH; the metal oxidic precursors were dissolved in the alcoholic solution with $Al(OC_4H_9)_3$, heated and kept at 60°C for about 20 min. $(NH_4)_6Mo_7O_{24}{\cdot}4H_2O$ was dissolved in a TPAOH aqueous solution. The alcoholic and the aqueous solutions were mixed together till the gel was formed (after 1 h at 80°C). It was aged at 21°C, dried (6 h, 100°C, in vacuum) and calcined (3 h, 550°C, air flow). The catalyst, obtained as a powder, was crushed and sieved (40–70 mesh). The Co/(Co + Mo) molar ratio was around 0.30 and the M/Al molar ratio was 0.1, except for CM–ZA, where Zr/Al was 0.15.

One 13.8 wt.% Co/SiO_2 sample was prepared by aqueous incipient wetness imbibition of Co nitrate on commercial SiO_2, specifically for XPS analysis.

2.2. Catalytic activity

The thiophene test allowed for a short time (3–10 h) catalyst screening. During HDS reaction, H_2 flowed (2 Nl/h) through a bubbling device containing thiophene at 5°C (vapour pressure of 4%). The reaction conditions were: $T = 300$°C, $P = 1$ bar, $38 < \text{WHSV} < 46$, $6\,h^{-1}$, catalyst weight = 1 g. The analyses of the HDS products were carried out by on-line GC − FPD + FID. The experimental error was below 3.3%. The extent of HDS and hydrogenation (HYD) activity (defined as the selectivity to butanes in the C_4 hydrocarbons derived from thiophene hydrogenation) were determined by the product distribution. The reaction scheme proposed for the thiophene conversion is reported in [9]. This test was not to evaluate the catalyst life.

2.3. Sulphidation procedure

The calcined samples were sulphided in a 10% H_2S/H_2 mixture (60 ml/min) at 400°C for 1 h (heating rate = 6°C/min); after cooling at 21°C in sulphiding mixture the sample was cleaned and kept in N_2 flow till characterisation.

2.4. Physico-chemical characterisation

Surface area measurements were performed by N_2 isotherm at −196°C with a Fisons Carlo Erba Sorptomatic 1990. The surface area was calculated with the BET method and the pore distribution with the Dollymore-Heal model. Before the analysis, the samples were treated at 300°C under vacuum (10^{-5} mbar), 4 h.

Adsorption measurements were performed in a pyrex volumetric apparatus equipped with pressure and vacuum detectors. Increasing amounts of adsorbate were added until saturation. The adsorbed amount of probe (μmol/g) was calculated by using the ideal gas law and the expansion coefficient of the system. The total number of acid sites was determined by ammonia adsorption at 150°C; the total number of the basic sites was determined by CO_2 adsorption at 21°C. The NO adsorption capacity was measured at 21°C. The experimental error is below 3%.

Before analysis the sulphided catalysts were treated at 350°C for 1 h in dynamic vacuum (10^{-5} mbar), the supports at 500°C for 1 h in dynamic vacuum (10^{-5} mbar).

TPD analysis was performed by the Pulse Chemisorb 2705 (Micromeritics). After activation at 500°C, 1 h, in He flow, the supports were contacted with pulses of pure CO_2 (or 10 vol.% NH_3/He) at 21°C. When the saturation was reached, a purge of the He flow at 21°C in 10 min was followed by increasing the temperature up to 500°C (heating rate = 20°C/min, He flow = 20 ml/min). Spectral deconvolution was performed by the Peak Solve (Galactic) program.

X-ray photoelectron spectroscopy (*XPS*) was performed with a VG Escalab MKII spectrometer, using non-monochromatized Al K_α radiation. Binding energies were referenced to the Al2p peak at 74 eV, i.e. Al2p in Al_2O_3. The binding energies and the peak shapes of Co2p and Mo3d allow determination of the oxidation state of the metals. Atomic ratios were obtained from the ratios of peak areas through appropriate sensitivity factors. The Co/Al and Mo/Al ratios reflect the dispersion of the metals on the support [10–12]. The binding energy of the S2p peak showed that only sulphides and no sulphates were present in all sulphided samples.

Table 1
Textural characteristics of the supports

Support	Composition	A_{sup} (m^2/g)	V_{pores} (cm^3/g)	Average diameter (Å)
A	Al_2O_3	319	0.38	<40
SA	SiO_2–Al_2O_3	314	0.38	50
ZA	ZrO_2–Al_2O_3	272	0.36	50
BA	B_2O_3–Al_2O_3	410	0.45	40
GA	Ga_2O_3–Al_2O_3	380	1.49	80

3. Results and discussion

The reference materials were Al_2O_3 (A) for the supports and $CoMo/Al_2O_3$ (CM–A) for the catalysts. All materials are amorphous at XRD analysis. The main characteristics (chemical analysis, surface area and pore volume determination) of supports and catalysts are reported in Tables 1 and 2, respectively. Surface area and pore volume of supports increase in the presence of B and Ga (Table 1). With regard to the addition of other oxides to the CoMo catalysts, the surface area does not change significantly, except for the sample containing B (Table 2). On the contrary, pore volume is always higher for $CoMo/Al_2O_3$ (1.24 cm^3/g) than for the modified catalysts. Except for CM–GA, catalysts have higher surface area and pore volume than respective supports, especially the one containing Zr (Tables 1 and 2).

The modification of the support composition affects its acid (able to bond NH_3) and basic (able to bond CO_2) properties as reported in Table 3. The nature of the metal oxide added to Al_2O_3 defines the acid–base distribution in the support. The amphoteric oxide (ZrO_2) increases the number of basic sites more than that of acid sites; Ga_2O_3 increases acidity more than basicity, while an acid oxide as B_2O_3 decreases the amount of basic sites and strongly increases the acid site density.

The acid and basic strength distribution was evaluated by TPD analysis. A diagram of the amounts of the probes (NH_3, CO_2) desorbed in each temperature range was evaluated by deconvolution analysis of the TPD profiles. The higher the desorption temperature, the higher is the site strength; the amount of probe not desorbed at 500°C corresponds to the amount of the strongest sites. In Figs. 1 and 2 the acid and basic strength distributions are depicted. Alumina shows a broad distribution of the acid and basic strength. The introduction of another metal oxide increases the acid strength of the materials and in particular the amount of the strong acid sites, able to retain ammonia at temperatures higher than 500°C (Fig. 1). The basicity is also influenced by the nature of the added metal oxide, because the relative amount of very weak, weak and medium basic sites changes (Fig. 2). On the basis of the site densities, the "acidity to basicity" ranking

Table 2
Textural characteristics of the catalysts

Catalyst	Support	Co (wt.%)	Mo (wt.%)	A_{sup} (m^2/g)	V_{pores} (cm^3/g)	Average diameter (Å)
CM–A	Al_2O_3	2.6	9.9	365	1.24	60
CM–SA	SiO_2–Al_2O_3	2.3	8.9	364	0.74	60
CM–ZA	ZrO_2–Al_2O_3	2.3	8.5	378	0.89	80
CM–BA	B_2O_3–Al_2O_3	2.5	9.1	475	1.12	60
CM–GA	Ga_2O_3–Al_2O_3	2.3	8.3	348	0.92	60

Table 3
NH_3, CO_2 and NO adsorption capacities of the supports and the catalysts

Calcined support	Acid site density (μmol/g)	Basic site density (μmol/g)	Chemisorbed NO (μmol/g)	Sulfided catalyst	Acid site density (μmol/g)	NO (μmol/g)
A	514	95	8	CM–A	588	85
SA	744	59	40	CM–SA	538	121
ZA	542	171	0	CM–ZA	490	95
BA	1058	21	309	CM–BA	646	393
GA	694	117	0	CM–GA	495	339

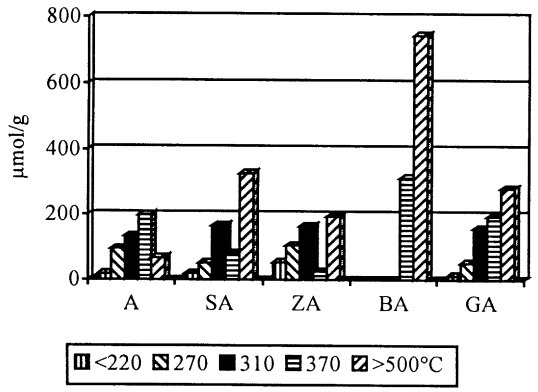

Fig. 1. Acid sites distribution of the supports.

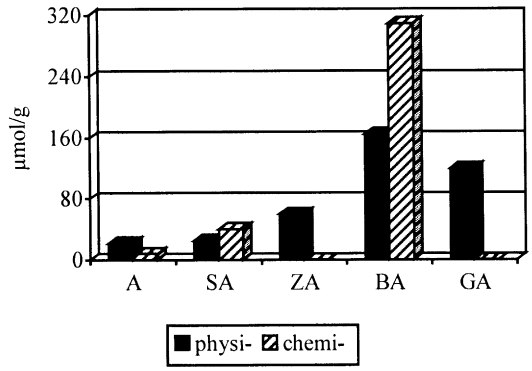

Fig. 3. Physi- and chemi-sorbed amount of NO on the supports.

of the supports follows the trend: BA > SA > A > GA > ZA.

The NO and NH_3 adsorption capacities in the sulphided samples are shown in Table 3. The density of acid sites in the catalysts is influenced by the nature of the added metal oxide, almost following the same trend found with the supports. In CM–A the presence of Co and Mo increases the acid sites density compared to the support. In the other catalysts a reverse behaviour is observed. The NO adsorption is higher in the mixed oxide systems than in the reference alumina catalyst; in particular CM–BA and CM–GA show an unusually high capacity to bond this probe.

The NO adsorption capacity is generally considered as a measure of the active CoMoS sites distribution in the traditional $CoMo/Al_2O_3$ materials [13]. The state of the art refers the interaction of NO with −OH groups of acidic materials, e.g. zeolites [14,15]. In order to evaluate if this kind of interaction is also present in our supports, volumetric measurements have been performed. The fraction of adsorbed NO able to withstand evacuation at 350°C is considered chemically bonded to the support. In Fig. 3 the physi- and chemi-sorbed amount of NO on the supports are depicted. NO is physisorbed on all supports in variable amount, while NO is chemisorbed only by the "more acidic" BA and SA materials. No differences in NO adsorption are observed in the sulphided supports with respect to the calcined ones.

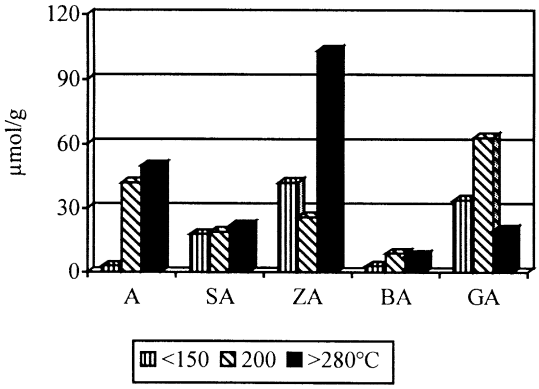

Fig. 2. Basic sites distribution of the supports.

The catalysts adsorb a higher NO amount than the corresponding supports. NO adsorption on the catalysts can be regarded as the sum of the contribution of the support (i.e. 8 µmol/g for A) and the supported CoMoS phase (i.e. $85 - 8 = 77$ µmol/g for CM–A). The contribution of the supported phase is roughly constant for all catalysts (ca. 80 µmol/g) but CM–GA, for which it is much higher (Table 3). This can be due either to a strong increase in the CoMoS dispersion or to a synergistic adsorption between CoMoS and Ga.

The differences in the NH_3 adsorption measurements of both supports and catalysts can be explained by the following model.

In CM–A, the introduction of Co and Mo precursors in the sol phase increases the "total" acidity of the catalyst after calcination. It is supposed that during gelling of the alumina matrix, the presence of another metal precursor causes a charge imbalance in the matrix [16]. The subsequent calcination causes the formation of "defects" in the network (i.e. Al–OH groups,

Table 4
XPS data on the sulphided catalysts

Catalyst	S/Al	Co/Al	Mo/Al	ΔE: Co2p−S2p (eV)	S/(Co + Mo)
CM–A	0.12	0.03	0.05	617.3	1.56
CM–SA	0.12	0.03	0.06	617.5	1.32
CM–ZA	n.d.[a]	n.d.	n.d.	n.d.	n.d.
CM–BA	0.13	0.03	0.06	617.7	1.38
CM–GA	0.24	0.04	0.08	618.0	1.94

[a] Not determined.

unsaturated Al sites, M–OH or unsaturated M sites), creating an acid character.

In a more complex mixed oxide system (CM–SA, CM–BA, CM–ZA, CM–GA), Co and Mo precursors can interact with the other component of the gelling matrix beside the alumina precursor. So far there is a lower contribution of the defects to the acidity, resulting in a lowering of the "total" acid sites density of the catalysts compared to the corresponding supports. After calcination this interaction is strengthened in agreement with the strength of the acid sites (i.e. following the Sanderson acid–base scale [17]).

XPS analysis has been performed to characterise the supported phase (Table 4). The reference sulphided Co/SiO_2 sample shows a binding energy difference of 616.5 eV between Co2p and S2p, in agreement with the presence of Co sulphide species. The binding energy difference of the catalysts (>617.3 eV) is significantly higher than that of Co/SiO_2 (616.5 eV). According to Alstrup et al. [18] this points out to the presence of the CoMoS active phase in the Al_2O_3 supported catalysts. As the Mo/Al and Co/Al ratios do not change significantly in all catalysts, except for CM–GA, the overall dispersion of CoMoS hardly seems to be affected by the changes in the support. CM–GA shows Co/Al and Mo/Al ratios higher by less than 30% than the other samples. Consequently this increase is not large enough to explain the much higher NO adsorption of CM–GA (Table 3). The intensity of the S2p peak is determined after subtraction of the contribution of Ga3s, which overlaps S2p: anyway the S/(Co + Mo) ratio of CM–GA is the highest. This may reflect a synergism between Co, Mo and Ga, which allow a more favourable sulphidation of the metals and therefore a stronger NO adsorption.

The catalytic performances of these materials are reported in Table 5. The HDS activity is lower in materials containing Zr or Ga. A correspondence between acid site density and HDS activity can be observed in Fig. 4. This increase in HDS activity can be caused by the favoured adsorption of thiophene on the acidic surface.

Table 5
Catalytic performances of the catalysts

Catalyst	HDS (%)	HYD (%)	HDS/HYD
CM–A	64.8	38.7	1.67
CM–SA	64.4	34.9	1.85
CM–ZA	41.7	30.8	1.35
CM–BA	66.0	31.3	2.11
CM–GA	45.8	29.8	1.54

A different relation is observed between acid site density and HYD (Fig. 4). An increase of the HYD activity as a function of the acid site density is observed in the low acidity range. The highest HYD activity is present in the standard CM–A, where the CoMoS active sites are not influenced by the changes of the surrounding environment, caused by the different oxides mixtures. A decrease in HYD activity

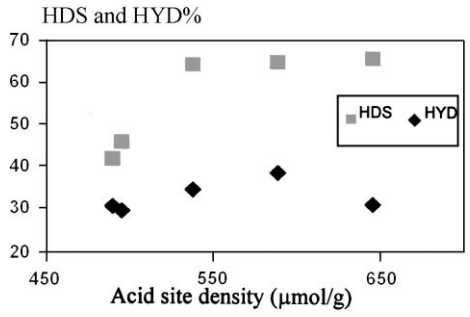

Fig. 4. Relation between the acid sites density (NH_3 adsorption) and HDS and HYD activities.

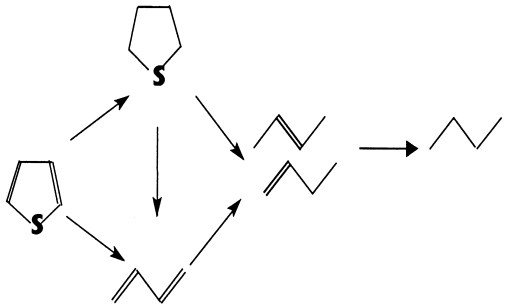

Fig. 5. Thiophene reaction scheme.

is observed in the most acidic CM–BA catalyst. This catalyst has the highest acid site density and acid strength. This behaviour is in agreement with the hypothesis that the strength of thiophene interaction via π-complexes depends on the acid strength of the surface [19]. In fact HYD is the consecutive reaction forming butanes from butadiene and butenes, produced by thiophene HDS (Fig. 5). When the interaction of these unsaturated products with the acid sites is too strong, the migration to CoMoS sites and the reactivity towards HYD are more difficult. Consequently, changing the composition of the catalysts by the addition of different oxides is advisable when a lower olefinic hydrogenation is required, e.g. naphtha.

4. Conclusions

Different oxidic precursors were introduced in the $CoMo/Al_2O_3$ system by the sol–gel method. The "acidity to basicity" ranking of the supports follows the trend: BA > SA > A > GA > ZA. The presence of Co and Mo precursors in the sol, influences the acid sites density of the catalysts by lowering its value in all mixed oxide systems. Due to the presence of the CoMoS phase in the whole series (as confirmed by XPS analysis) and since NO adsorption is considered as a measure of the CoMoS phase availability, the presence of a second metal oxide in the system does not seem to influence its availability, except in the Ga containing catalyst. The addition of another oxide in the catalytic system influences HDS and HYD activities in thiophene reaction test. A relation between the density of acid sites and HDS activity is found in these materials.

Acknowledgements

The authors gratefully thank Dr. F. Bazzano, Dr. D. Berti and Mr. L. Galasso of EniTecnologie and Dr. L. Meda of Istituto Donegani–EniChem for their helpful contribution to the experimental work.

References

[1] T. Sutikno, Oil Gas J. June 7th, 1999, 55
[2] K. Arata, Adv. Catal. 37 (1990) 165.
[3] K. Tanabe, M. Misono, Y. Ono, H. Hattori, Stud. Surf. Sci. Catal. 51 (1989) 1.
[4] E. Lecrenay, K. Sakanishi, I. Mochida, T. Suzuka, Appl. Catal. 175 (1998) 237.
[5] M.P. Borque, A. Lopez-Agudo, E. Olguin, M. Vrinat, L. Cedeno, J. Ramirez, Appl. Catal. 180 (1999) 53.
[6] Y.-W. Chen, M.-C. Tsai, Catal. Today 50 (1999) 57.
[7] S. Peratello, G. Bellussi, V. Calemma, Eniricerche SpA, Eur. Patent 0748652 (1996).
[8] L. Lebihan, C. Mauchaussé, L. Duhamel, J. Grimblot, J. Sol–Gel Sci. Technol. 2 (1994) 837.
[9] M.R. Blake, M. Eyre, R.B. Moyes, P.B. Wells, Bull. Soc. Chim. Belg. 90 (1981) 1293.
[10] J.F. Moulder, W.F. Stickle, P.E. Sobol, K.D. Bomben, Handbook of X-ray Photoelectron Spectroscopy, Perkin Elmer, Eden Prairie, 1992.
[11] D. Briggs, M.P. Seah, Practical Surface Analysis, Vol. 1, Wiley, Chichester, UK 1990.
[12] J.W. Niemantsverdriet, Spectroscopy in Catalysis, VCH, Weinheim, 1995.
[13] L. Portela, P. Grange, B. Delmon, Catal. Rev. Sci. Eng. 37 (1995) 699.
[14] T.E. Hoost, K.A. Laframboise, K. Otto, Catal. Lett. 33 (1995) 105.
[15] A. Satsuma, M. Iwase, A. Shichi, T. Hattori, Y. Murakami, Stud. Surf. Sci. Catal. 105 (1997) 1533.
[16] J.B. Miller, E.I. Ko, Catal. Today 35 (1997) 269.
[17] R.T. Sanderson, Inorganic Chemistry, Reinhold, New York, 1966 (Chapter 12).
[18] I. Alstrup, I. Chorkendorff, R. Candia, B.S. Clausen, H. Topsoe, J. Catal. 77 (1982) 397.
[19] H.C. Lee, J.B. Butt, J. Catal. 49 (1977) 320.
[20] Y.C. Park, H.-K. Rhee, Appl. Catal. 179 (1999) 145.